

# Crossover from Coulomb blockade to quantum Hall effect in suspended graphene nanoribbons

Dong-Keun Ki and Alberto F. Morpurgo\*

*Département de Physique de la Matière Condensée (DPMC) and Group of Applied Physics (GAP),  
University of Geneva, 24 Quai Ernest-Ansermet, CH1211 Genève 4, Switzerland*

(Dated: August 15, 2018)

Suspended graphene nano-ribbons formed during current annealing of suspended graphene flakes have been investigated experimentally. Transport measurements show the opening of a transport gap around charge neutrality due to the formation of "Coulomb islands", coexisting with quantum Hall conductance plateaus appearing at moderate values of magnetic field  $B$ . Upon increasing  $B$ , the transport gap is rapidly suppressed, and is taken over by a much larger energy gap due to electronic correlations. Our observations show that suspended nano-ribbons allow the investigation of phenomena that could not so far be accessed in ribbons on  $\text{SiO}_2$  substrates.

PACS numbers: 72.80.Vp,73.43.Qt,73.23.Hk,85.35.-p

Theoretical studies indicate that in graphene nano-ribbons (GNRs) –long and narrow graphene channels– Dirac electrons should give origin to a number of unique phenomena, accessible in transport experiments. Examples include the controlled opening of a band gap [1], the realization of gate-tunable magnetic states [2], or the interplay between Landau and size quantization [3]. Theories, however, usually consider disorder-free GNRs with idealized edge structure [1–3], whereas disorder is invariably present in experimental systems, which leads to the formation of localized states in a wide energy range [4–6]. In the presence of strong disorder, transport through GNRs near charge neutrality is mediated by hopping, and GNRs behave as an ensemble of randomly assembled quantum dots, resulting in the opening of a so-called transport gap [4–6]. In this regime, even the most basic manifestations of the Dirac character of electrons, such as the half-integer conductance quantization in a magnetic field [7], are washed out [5, 6].

A complete elimination of disorder would require control of the edge structure [8, 9], and the fabrication of suspended GNR devices to avoid the influence of substrate-induced disorder [10]. The high electronic quality of suspended graphene devices has indeed been demonstrated –among others– by the observation of ballistic transport [10, 11] and of the fractional quantum Hall effect in monolayers [12, 13], and of small interaction induced gaps in bilayers [14]. Crucial to achieve high-quality is a current annealing step, i.e., forcing a large current to heat graphene, in order to desorb adsorbates from the surface [10, 15]. The large current required can lead to cleavage of graphene, which usually results in device failure. We have found that in several cases a partial graphene cleavage can occur [11, 16], leading to the formation of narrow suspended nano-ribbons.

Here, we report on magneto-transport measurements through a device produced in this way. We find that, while a disorder-induced transport gap still opens around charge neutrality (as observed in lithographically defined

GNRs on  $\text{SiO}_2$  substrates [4–6]), Coulomb blockade is strongly suppressed by the application of only a moderate magnetic field ( $B \approx 2$  T) [6, 8]. This leads to quantum Hall conductance plateaus at finite carrier density, and the occurrence of a strongly insulating state (with a gap increasing with magnetic field) around charge neutrality [17]. These phenomena, normally observed only in sufficiently clean graphene [10–13], indicate that suspension of GNRs result in a significant improvement of their electronic quality, enabling the observation of phenomena not accessible in GNRs on  $\text{SiO}_2$  substrates [4–6, 8].

Wide suspended graphene devices are fabricated using polydimethylglutarimide (PMGI) resist (LOR, MicroChem) as a sacrificial supporting layer, as described by Tombros *et al.* (see Ref. 18 for details). Measurements are performed in a two-terminal configuration with Ti/Au contacts (10/70 nm) separated by a distance of approximately 0.5-1  $\mu\text{m}$  (depending on the device), using the highly doped Si substrate as gate electrode (approximately 1  $\mu\text{m}$  away from graphene). The inset in Fig. 1(a) shows a scanning electron microscope (SEM) image of a successfully annealed device.

Current annealing was performed by slowly ramping up the bias voltage  $V$  to  $\sim 1$ -2 V (depending on the specific sample) in vacuum at 4.2 K, and maintaining the applied bias for extended periods of time. For most devices, this procedure had to be repeated several times before a sharp resistance peak at approximately zero gate voltage ( $V_g = 0$  V) could be observed (see Figs. 1(a),(b)). In successfully annealed devices, low-field integer quantum Hall effect with a complete lifting of spin and valley degeneracy was observed, together with a strongly insulating state appearing at charge neutrality upon the application of a magnetic field  $B$  (see Figs. 1(c),(d)). These observations and the narrow width of the resistance peak around charge neutrality ( $\simeq 10^{10} \text{ cm}^{-2}$ ) indicate the high device quality [10–13].

In several different devices, we observed sudden, large increases in resistance during annealing, originating from

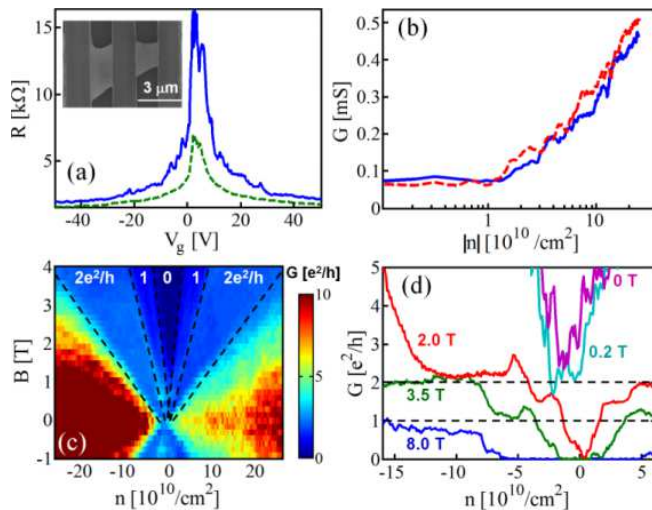


FIG. 1: (Color online) (a) Two-terminal resistance ( $R$ ) versus  $V_g$  of the wide suspended graphene device shown in the inset, measured at  $T = 0.24$  K (blue line) and 2.0 K (Green dashed line). (b) Semi-log plot of the conductance  $G$  measured at 0.24 K, as a function of carrier density  $n$  for both electrons (blue solid line) and holes (red dashed line). The resistance peak width is approximately  $10^{10}$  carriers/cm<sup>2</sup>. (c) Conductance  $G$  as a function of carrier density  $n$  and magnetic field  $B$ , showing well defined quantum Hall states with  $G = 1$  and  $2e^2/h$ , and an insulating state around charge neutrality. (d)  $G(n)$  at different values of  $B$  selected from (c), zooming in on quantum Hall plateaus; the dashed lines correspond to  $G = 1$  and  $2e^2/h$ .

partial breaking of the graphene layer (see, e.g., Fig. 2(a)). In these cases, the measured  $V_g$  dependence of the conductance  $G$  exhibits features that are characteristically observed in nano-ribbons [4–6]. Figs. 2(b)-(d) show data from a device in which the phenomenon was seen more clearly. Specifically Fig. 2(b) shows the  $V_g$  dependence of the conductance before (green curve) and after (blue curve) a final annealing step, which resulted in the opening of a transport gap in the  $V_g$  range between 0 and 20 V. In this range, a random sequence of conductance peaks is observed (Fig. 2(c)), and measurements of the differential conductance versus  $V$  and  $V_g$  show “Coulomb diamonds” characteristic of a disordered array of quantum dots (Fig. 2(d)). This is the same behavior observed in GNRs on SiO<sub>2</sub> substrates [4–6].

Measurements as a function of  $B$  illustrate the difference between suspended GNRs and GNRs on SiO<sub>2</sub> [5, 6, 8]. Fig. 3(a) shows the  $V_g$  and  $B$  dependence of the conductance, where quantum Hall states with  $G = 2e^2/h$  are observed for holes and for electrons. The quantization of the conductance is better seen in Fig. 3(b), which shows cuts at fixed  $B$  of the color plot in Fig. 3(a). For negative  $V_g$ , the plateaus appear at  $B \simeq 2 - 2.5$  T, whose conductance is very close to  $2e^2/h$  ( $\sim 1.9e^2/h$ ; the deviation is due to a 350  $\Omega$  contact resistance) as expected for Dirac electrons [7]. For positive gate volt-

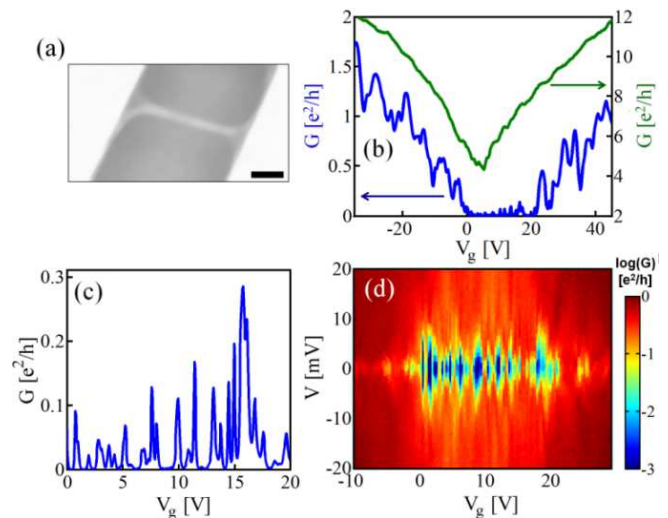


FIG. 2: (Color online) (a) SEM image of a GNR formed while annealing a suspended graphene layer (the bar is 100 nm long). (b) Gate dependence of the differential conductance  $G = \frac{dI}{dV}(V_g)$  measured after a first annealing step of a suspended graphene device (green line on top) and after a second step (blue line at the bottom), in which a suspended GNR is formed. Panel (c) zooms in on the transport gap region of (b), and shows resonances due to Coulomb blockade. (d)  $\log(G)$  as a function of bias  $V$  and gate  $V_g$  voltages, showing the Coulomb diamonds characteristically seen in GNRs. All data are taken at 4.2 K.

ages, the plateaus become well defined only at larger magnetic field (see Fig. 3(d)) [19]. Around charge neutrality and for  $B > 2$  T, a strongly insulating state is seen, similarly to what is normally observed in large, clean suspended graphene flakes [12, 13], originating from interaction-induced electronic correlations [17].

To further test the quantum Hall nature of the plateaus we plot the conductance  $G$  as a function of filling factor  $\nu = n\phi_0/B$  (with  $\phi_0 = h/e$  and  $n$  carrier density), to check if all data collapse on a single curve as expected. To extract the carrier density  $n$  as a function of  $V_g$ , we exploit the fact that at the center of a  $2e^2/h$  conductance plateau at a fixed magnetic field  $B$ ,  $\nu = 2$  (owing to spin degeneracy) so that  $n = 2\phi_0/B$ . We then find that the carrier density scales linearly with gate voltage, as it should. The slope  $\alpha = \Delta n/\Delta V_g = 7.8 \times 10^9 \text{ cm}^{-2}\text{V}^{-1}$  is slightly larger than the value,  $4.7 \times 10^9 \text{ cm}^{-2}\text{V}^{-1}$ , estimated from the formula for a parallel plate capacitor, as expected, since the ribbon width [19] is smaller than the distance to the gate (the value of  $\alpha$  agrees quantitatively with a recent study of suspended graphene in the quantum Hall regime [20], where an enhanced capacitance at the edges was found). By extrapolating to  $B = 0$  T, we find that charge neutrality occurs at  $V_g = V_{CNP} = 8.5$  V (see Fig. 3(c)). Using this relation between  $n$  and  $V_g$ , we plot the conductance as a function of  $\nu$  in the  $B$  range between 5.0 and 8.0 T (Fig. 3(d)). On the hole side all

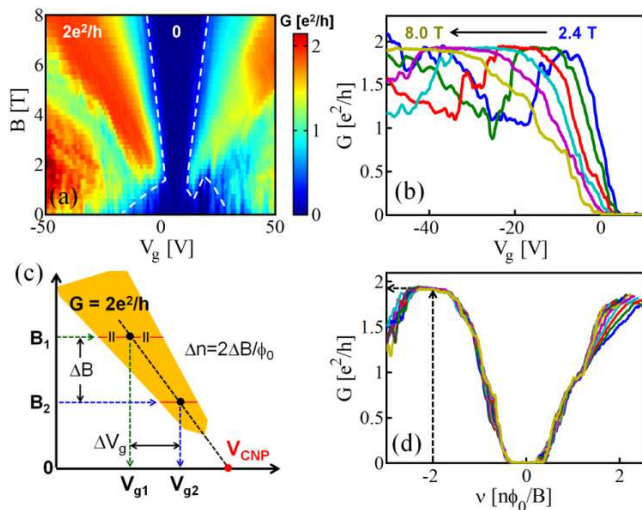


FIG. 3: (Color online) (a) Color plot of  $G(V_g, B)$ , with quantized conductance values indicated. The broken line is guide to the eye, separating the conducting and insulating regions as a function of  $V_g$  and  $B$ . (b)  $G(V_g)$  at  $B = 2.4$  T, 3.4 T, 4.4 T, 5.4 T, 6.5 T, and 8.0 T (from the right to the left, respectively), showing conductance plateaus for hole accumulation. (c) Schematic view of the procedure followed to estimate  $V_{CNP}$  and  $\alpha (\equiv \Delta n / \Delta V_g)$  described in the text. (d)  $G$  as a function of the filling factor  $\nu (\equiv n\phi_0/B)$  in the magnetic field range between 5.0 and 8.0 T: all different measurements tend to collapse on a single curve. The presence of  $2e^2/h$  conductance plateaus for electron accumulation becomes apparent in this plot. All data are taken at 4.2 K.

curves collapse together nearly perfectly; on the electron side the trend is similar, and although the collapse is not as good, the presence of a  $2e^2/h$  quantum Hall plateau becomes apparent.

We conclude that in suspended GNRs the transport gap due to Coulomb islands at  $B = 0$  T coexists, at  $B > 2$  T, with quantum Hall effect at finite carrier density, and with a large-gap correlated state around charge neutrality. As these phenomena occur at low magnetic field only when the level of disorder is sufficiently low [10–13], their observation indicates that the quality of suspended GNRs created during current annealing is considerably better than that of GNRs on  $\text{SiO}_2$  substrates [4–6, 21]. Similarly to larger suspended graphene devices, the low disorder level in suspended GNRs is due to the absence of a substrate and to the current annealing. The current-induced cleaving process—which occurs in vacuum—may also lead to better edges [22] as compared to lithographically defined GNRs [4–6].

The higher quality enables the investigation of the competition between Coulomb blockade—originating from geometrical confinement in the presence of disorder—and the quantum-Hall effect, due to magnetic confinement. One interesting aspect is the dependence of the transport gap on magnetic field. Fig. 3(a) shows that the transport gap due to Coulomb islands (i.e., the  $V_g$

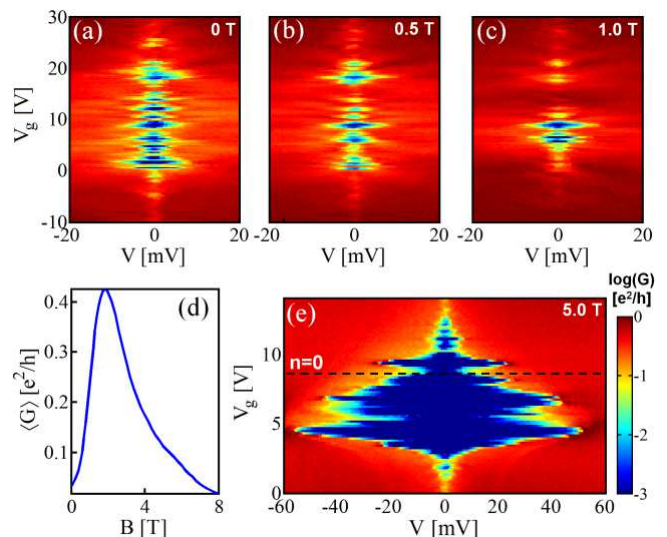


FIG. 4: (Color online) (a-c) From left to right, logarithm of the differential conductance  $G = \frac{dI}{dV}$  versus  $V$  and  $V_g$ , for  $B = 0$  T, 0.5 T, and 1 T: increasing  $B$  causes a decrease of the  $V_g$  interval in which Coulomb diamonds dominate low-bias transport. (d) Conductance averaged in  $V_g$ 's between 0 V and 20 V,  $\langle G \rangle$ , as a function of  $B$ . At  $B > 2$  T,  $\langle G \rangle$  decreases due to the large, correlation-induced gap around the charge neutrality, which becomes larger as  $B$  increases. (e)  $\log(G)$  versus  $V$  and  $V_g$  at  $B = 5.0$  T, showing the opening of a large gap around charge neutrality due to electronic correlations (the color scale in the legend is the same for all panels). The broken line at  $V_g = 8.5$  V corresponds to  $V_{CNP}$  extracted from the quantum Hall effect analysis (see Fig. 3(c)). All data are taken at 4.2 K

interval where the conductance is strongly suppressed) narrows down with increasing  $B$  from 0 to 1 T. The phenomenon is illustrated in more detail in Figs. 4(a)-(c), which show measurements of Coulomb diamonds for different values of  $B$ . While at  $B = 0$  T diamonds appear when  $V_g$  is between 0 and  $\simeq 20$  V, at  $B = 1$  T they are only present between  $\simeq 5$  and 10 V. Correspondingly, the conductance  $\langle G \rangle$  averaged over  $V_g$  between 0 V and 20 V increases by more than ten times as  $B$  is increased from 0 to  $\sim 2$  T (Fig. 4(d)). An increase in the averaged conductance was found previously in GNRs on  $\text{SiO}_2$  substrates [6, 8], and correctly attributed to a magnetic-field induced increase of the electron localization length, but a full crossover from a Coulomb blocked regime to fully developed conductance quantization has not been observed previously [5, 6, 8, 21].

Note that, at low carrier density, a large increase in the two-terminal conductance of a narrow disordered wire (i.e. where at  $B = 0$  T electron states are localized) upon entering the quantum Hall regime is a manifestation of the Dirac fermion character of the charge carriers. If electrons were described by the Schrodinger equation—as it would be the case for a narrow wire defined in a conventional two-dimensional electron gas—entering the

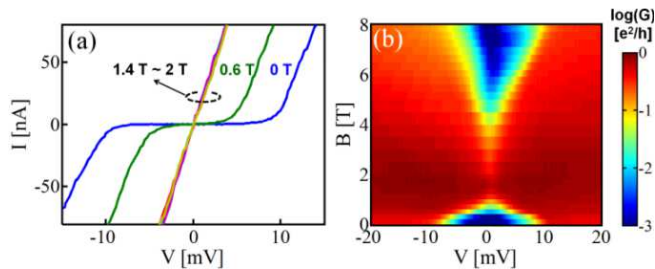


FIG. 5: (Color online) (a)  $I - V$  characteristics of the device at  $V_g = 1.4$  V (at  $B = 0$  T, 0.6 T and in the range between 1.4 T and 2.0 T, as indicated). (b) Logarithm of the differential conductance  $G = \frac{dI}{dV}$  versus  $V$  and  $B$  for  $V_g = 1.4$  V away from the charge neutrality, showing the closing of the transport-gap with increasing  $B$  (the lo-bias conductance suppression above 4 T is due to the insulating state around the charge neutrality). All data are taken at 4.2 K.

quantum Hall regime at low carrier density would result in a so-called sub-band depopulation (due to the enhanced magnetic field confinement), and in a decrease of the two terminal conductance with increasing  $B$  [23]. For Dirac electrons, the existence of a zero-energy Landau level is responsible for this difference, and causes the conductance to increase.

The crossover from the Coulomb-blockaded regime at  $B = 0$  T –characterized by non-Ohmic  $I - V$  curves– to a linear transport regime at finite magnetic field  $B$  (see Fig. 5(a)) is also apparent in measurements at fixed  $V_g$  in the “transport gap” range. Fig. 5(b) shows data taken at  $V_g = 1.4$  V, in which a 10 meV gap due to charging energy at  $B = 0$  T closes when  $B$  is increased to 1.4 T (at  $B > 4$  T,  $G$  decreases again due to the large gap associated to the correlated state around the charge neutrality point). The full suppression of Coulomb blockade is expected in GNRs exhibiting a clear quantum-Hall effect, since plateaus with quantized conductance (Fig. 3) indicate that transport is mediated by edge states and that backscattering is absent. This implies that electrons are delocalized over the full device length, so that transport is not any more blocked by the Coulomb charging energy associated to localized states in “disorder-induced islands”.

Finally, we discuss the crossover –at charge neutrality– between the transport gap due to Coulomb islands, and the gap at large  $B$  values. The transport gap associated to Coulomb islands is not a “true” gap in the density of states, i.e. states are still present at low energy. On the contrary, the strongly insulating state appearing for  $B > 1$  T seems to have a true gap, since no current can be detected at low bias over a large  $V_g$  range (Fig. 4(e)). Contrary to the transport gap associated to Coulomb blockade, this gap increases with increasing  $B$  (see Fig. 3(a) and Fig. 5(b)) and at sufficiently large  $B$ , it behaves virtually identically to what is found in clean suspended layers of larger width (see Fig. 2(c)) [12, 13]. Note that,

as observed in Ref. 13, the correlation induced gap in Fig. 4(e) is asymmetric around the charge neutrality point, i.e., electron-hole symmetry is broken in the underlying electronic state .

We conclude by comparing our results to those of Ref. 11, where Tombros *et al.* realized a constriction by annealing a suspended graphene flake, and observed signatures of conductance quantization (i.e. ballistic transport) at  $B = 0$  T, whereas at  $B = 0$  T we observe carrier localization. What appears to be mainly responsible for the different behavior is the device length. In Ref. 11 the length of the constriction is comparable to (or shorter than) the width; in all devices imaged by us, the length of the structures is much longer than their width. Edge scattering is therefore much more severe, resulting in electron localization and preventing ballistic transport. It is clear that systematic investigations of suspended devices as a function of their width and length are worth pursuing, to explore the properties of confined Dirac electrons in different transport regimes. Such a study would provide information on the mechanisms of edge scattering and on the nature of edge disorder, two virtually unexplored aspects of graphene nanostructures. A difficulty is the lack of control of the dimensions of the structures that are created by current annealing, and it will be crucial to make the fabrication process more controllable (e.g., by “seeding” structural defects in the graphene layer before suspension, where annealing-induced cleavage occurs preferentially). Even without this control, our results show that nano-ribbons generated by annealing suspended graphene enable the observation of new and interesting phenomena.

We acknowledge N. Tombros for discussions about device fabrication and A. Ferreira for technical support. Financial support from the NCCRs MANEP, and QSIT, and from SNF is gratefully acknowledged.

---

\* Electronic address: Alberto.Morpurgo@unige.ch

- [1] K. Nakada, M. Fujita, G. Dresselhaus, and M. S. Dresselhaus, *Phys. Rev. B* **54**, 17954 (1996); L. Brey and H. A. Fertig, *Phys. Rev. B* **73**, 235411 (2006); Y. W. Son, M. L. Cohen, and S. G. Louie, *Phys. Rev. Lett.* **97**, 216803 (2006).
- [2] Y. W. Son, M. L. Cohen, and S. G. Louie, *Nature* **444**, 347 (2006); O. V. Yazyev, *Rep. Prog. Phys.* **73**, 056501 (2010).
- [3] N. M. R. Peres, A. H. Castro Neto, and F. Guinea, *Phys. Rev. B* **73**, 241403(R) (2006); A. A. Shylau, I. V. Zozoulenko, H. Xu, and T. Heinzl, *Phys. Rev. B* **82**, 121410(R) (2010); A. A. Shylau and I. V. Zozoulenko, *Phys. Rev. B* **84**, 075407 (2011).
- [4] M. Y. Han, B. Özyilmaz, Y. Zhang, and P. Kim, *Phys. Rev. Lett.* **98**, 206805 (2007); C. Stampfer *et al.*, *Phys. Rev. Lett.* **102**, 056403 (2009); M. Y. Han, J. C. Brant, and P. Kim, *Phys. Rev. Lett.* **104**, 056801 (2010); P.

- Gallagher, K. Todd, and D. Goldhaber-Gordon, Phys. Rev. B **81**, 115409 (2010); S. Dröscher, H. Knowles, Y. Meir, K. Ensslin, and T. Ihn, Phys. Rev. B **84**, 073405 (2011).
- [5] F. Molitor *et al.*, Phys. Rev. B **79**, 075426 (2009); S. Schmidmeier *et al.*, arXiv:1111.4330 (unpublished).
- [6] J. B. Oostinga, B. Sacépé, M. F. Craciun, and A. F. Morpurgo, Phys. Rev. B **81**, 193408 (2010); J. Bai *et al.*, Nature Nanotech. **5**, 655 (2010).
- [7] K. S. Novoselov *et al.*, Nature (London) **438**, 197 (2005); Y. Zhang, Y. W. Tan, H. L. Stormer, and P. Kim, Nature (London) **438**, 201 (2005).
- [8] J. M. Poumirol *et al.*, Phys. Rev. B **82**, 041413(R) (2010).
- [9] L. Jiao, X. Wang, G. Diankov, H. Wang, and H. Dai, Nature Nanotech. **5**, 321 (2011); T. Shimizu *et al.*, Nature Nanotech. **6**, 45 (2011); X. Wang *et al.*, Nature Nanotech. **6**, 563 (2011); M. W. Lin *et al.*, Phys. Rev. B **84**, 125411 (2011); M. W. Lin *et al.*, Nanotech. **22**, 265201 (2011).
- [10] X. Du, I. Skachko, A. Barker, and E. Y. Andrei, Nature Nanotech. **3**, 491 (2008); K. I. Bolotin *et al.*, Solid State Commun. **146**, 351 (2008).
- [11] N. Tombros *et al.*, Nature Phys. **7**, 697 (2011).
- [12] X. Du, I. Skachko, F. Duerr, A. Luican, and E. Y. Andrei, Nature (London) **462**, 192 (2009)
- [13] K. I. Bolotin, F. Ghahari, M. D. Shulman, H. L. Stormer, and P. Kim, Nature (London) **462**, 196 (2009).
- [14] R. T. Weitz, M. T. Allen, B. E. Feldman, J. Martin, and A. Yacoby, Science **330**, 812 (2010); F. Freitag, J. Trbovic, M. Weiss, and C. Schönberger, Phys. Rev. Lett. **108**, 076602 (2012); J. Velasco Jr *et al.*, Nature Nanotech. **7**, 156 (2012); A. Veligura *et al.*, arXiv:1202.1753 (unpublished).
- [15] J. Moser, A. Barreiro, and A. Bachtold, Appl. Phys. Lett. **91**, 163513 (2007).
- [16] J. Moser and A. Bachtold, Appl. Phys. Lett. **95**, 173506 (2009).
- [17] J. G. Checkelsky, L. Li, and N. P. Ong, Phys. Rev. Lett. **100**, 206801 (2008); Phys. Rev. B **79**, 115434 (2009); M. O. Goerbig, Rev. Mod. Phys. **83**, 1193 (2011).
- [18] N. Tombros *et al.*, J. Appl. Phys. **109**, 093702 (2011).
- [19] It has not been possible to image all the nano-ribbons produced by annealing, because most devices broke in the course of the experiments, which gives an uncertainty about their dimensions. In the cases that we could image, the nano-ribbon length was comparable to the contact separation (see Fig. 2(a)). For the nano-ribbon whose data we show here the width  $W$  can be estimated from the results of the measurements. Quantum Hall plateaus starting at 2-2.5 T indicates that  $W > 100$  nm, since otherwise the edge states at opposite edges would overlap, preventing the observation of conductance quantization. By comparing the charging energy ( $\approx 10$  meV, see Fig. 2(d)) to data measured in ribbons on SiO<sub>2</sub> –and given that the dielectric constant of SiO<sub>2</sub> partially screens Coulomb interactions– we also estimate that  $W < 200$  nm.
- [20] I. J. Vera-Marun *et al.*, arXiv:1112.5462 (unpublished).
- [21] R. Ribeiro *et al.* [Phys. Rev. Lett. **107**, 086601 (2011)], observed  $2e^2/h$  quantum-Hall conductance quantization in a GNR, but only at high field, in pulsed magnetic field experiments. In those experiments, no clear evidence of the correlation induced gap around charge neutrality was found even at  $B = 55$  T.
- [22] X. Jia *et al.*, Science **323**, 1701 (2009).
- [23] C. W. J. Beenakker and H. van Houten, Solid State Physics **44**, 1 (1991).